



Published in final edited form as:

Stem Cells. 2008 October ; 26(10): 2666–2673. doi:10.1634/stemcells.2008-0270.

IFATS Series: Stem Cell Antigen-1 Positive Ear Mesenchymal Stem Cells (EMSC) Display Enhanced Adipogenic Potential

Jaroslaw Staszkieicz^{1,3}, Jeffrey Gimble², Jessica A. Manuel¹, and Barbara Gawronska-Kozak¹

¹Regenerative Biology Laboratory, Pennington Biomedical Research Center, Louisiana State University System, Baton Rouge, Louisiana, USA ²Stem Cell Biology, Pennington Biomedical Research Center, Louisiana State University System, Baton Rouge, Louisiana, USA ³Department of Animal Physiology, Warmia & Mazury University in Olsztyn, Olsztyn, Poland

Abstract

Hyperplasia is a major contributor to the increase in adipose tissue mass that is characteristic of obesity. However, the identity and characteristics of cells that can be committed into adipocyte lineage remains unclear. Stem cell antigen 1 (Sca-1) has been used recently as a candidate marker in the search for tissue-resident stem cells. In our quest for biomarkers of cells that can become adipocytes, we analyzed ear mesenchymal stem cells (EMSC) that can differentiate into adipocytes, osteocytes, chondrocytes and myocytes. Our previous studies have demonstrated that EMSC abundantly expressed Sca-1. In the present study, we have analyzed the expression of adipogenic transcription factors and adipocyte-specific genes in Sca-1 enriched and Sca-1 depleted EMSC fractions. We found that Sca-1 enriched but not Sca-1 depleted EMSC showed a greater accumulation of lipid droplets during adipogenic differentiation. Similarly, EMSC isolated from Sca-1^{-/-} mice displayed reduced lipid accumulation relative to EMSC from wild type controls ($p < 0.01$). Comparative analysis of the adipogenic differentiation process between Sca-1 enriched and Sca-1 depleted population of EMSC revealed substantial differences in the gene expression. Pref-1, C/EBP β , C/EBP α , PPAR γ 2, LPL and aP2 were expressed at significantly higher levels in Sca-1 enriched EMSC fraction. However the most striking observation was that leptin was detected only in the conditioned media of Sca-1 enriched EMSC. Additionally, we performed loss-of-function (Sca-1 morpholino antisense oligonucleotides) experiments. The presented data suggest that Sca-1 is a biomarker for EMSC with the potential to become functionally active adipocytes.

Keywords

Sca-1; mesenchymal stem cells; Adipogenesis; Differentiation; Sca-1

© 2008 AlphaMed Press

Correspondence: Barbara Gawronska-Kozak, Ph.D., Pennington Biomedical Research Center, Louisiana State University System, 6400 Perkins Rd., Baton Rouge, Louisiana 70808, USA. Telephone: 225-763-0254; Fax: 225-763-0273; KozakB@pbrc.edu; website: www.pbrc.edu.

Author contributions: J.S.: conception and design, collection and assembly of data, data analysis and interpretation, manuscript writing, final approval of manuscript; J.M.G.: conception and design, data analysis and interpretation, manuscript writing, final approval of manuscript; J.A.M.: collection and assembly of data, final approval of manuscript; B.G.-K.: conception and design, administrative support, collection and assembly of data, data analysis and interpretation, manuscript writing, final approval of manuscript.

INTRODUCTION

We have previously established and characterized a primary culture of mouse ear mesenchymal stem cells (EMSC) that are isolated from the external murine ears [1]. These cells have the characteristics of stem cells including the ability to self-renewal and to differentiate into various types of cells at the clonal level [1–3]. Immunophenotype analyses of EMSC showed that undifferentiated EMSC are strongly positive for the Sca-1, and are negative for hematopoietic markers (CD45, CD4) [2]. Furthermore, we found robust accumulation of lipid droplets in Sca-1 enriched (Sca-1⁺), but not depleted (Sca-1⁻) EMSC fractions exposed to an adipogenic induction medium. These observations have led us to postulate that Sca-1 plays a role in adipogenic differentiation.

A substantial body of literature links Sca-1 to stem cell function. Also known as a Ly-6A/E, Sca-1 is an 18-kDa glycosyl phosphatidylinositol-anchored cell surface protein initially identified as an antigenic marker of murine hematopoietic cells [4]. Sca-1 has been detected on bone marrow-derived mesenchymal stem cells [5–8], skeletal muscle stem cells [9], mammary epithelial stem cells [10], cardiac tissue [11], skin [12], muscle [13–18], kidney [19], testis [20], liver [21,22], prostate [23,24], and pulmonary endothelium [25]. Sca-1 is linked to the self-renewal of mesenchymal [26] and hematopoietic [27] progenitors in the bone marrow and myogenic stem cells [28]. Additionally, it has been reported that skeletal muscle-derived and bone marrow-derived mesenchymal stem cells expressing Sca-1 can differentiate into cardiomyocytes *in vivo* [6], and contribute to muscle regeneration [29], respectively. Myogenic and endothelial cell progenitors identified in the interstitial spaces of murine skeletal muscle, which are strongly positive for Sca-1, display the potential to differentiate into adipocytes, endothelial, and myogenic cells [18]. Moreover, a population of Sca-1⁺ cells has been identified in neonatal mouse skin that expresses adipocyte markers [30]. These observations are consistent with our EMSC observations.

To test our hypothesis that Sca-1 plays a role in adipogenic differentiation, we have compared the adipogenic capacity of Sca-1 enriched vs. Sca-1 depleted populations of EMSC using both antibody-based sorting and loss-of-function experiments. As parameters for this *in vitro* evaluation, we have examined the expression of adipogenic transcription factors and adipocyte expressed genes, Oil red O staining, BODIPY staining and leptin protein secretion.

MATERIALS AND METHODS

Animals

C57BL/6J mice at the age of 3–6 weeks were used in the study. Experiments involving animals were approved by the Pennington Biomedical Research Center Institutional Animal Care and Use Committee in accordance with NIH guidelines. All procedures were designed to minimize the suffering of experimental animals. Mice were housed in a temperature- and humidity-controlled room (22 ± 2°C and 30–70%, respectively) with a 12-h light/12-h dark cycle (lights on at 0600 h) and were given ad libitum access to chow diet and tap water throughout the study. Mice were sacrificed by CO₂ asphyxiation followed by cervical dislocation.

Cell Harvest and Culture

For isolation of EMSC, outer ears were excised, minced and digested with collagenase type I (2 mg/1 ml; Worthington Biochemical, Freehold, NJ) in a shaking bath for 1h at 37°C. The cell suspension was filtered through a 70 µm cell strainer (Becton Dickinson Labware, NJ) followed by centrifugation (360 × g, 5 min, RT). Pelleted cells were resuspended in 1 ml red blood lysis buffer (Sigma Co., St. Louis, MO) and centrifuged as above. The isolated cells were plated in 100 mm Petri dishes (p = 0) in Dulbecco's Modified Eagle Medium (DMEM/

F12; Invitrogen, Carlsbad, CA) supplemented with 1% antibiotic solution and 15% fetal bovine serum (FBS; Invitrogen, Carlsbad, CA). Subconfluent primary cultures were trypsinized (0.05% trypsin/0.53 mM EDTA; Life Technologies, New York, NY) followed by immunomagnetic cell sorting.

Sca-1 Magnetic Sorting

Magnetic labeling cell sorting with anti Sca-1 immunomagnetic microbeads (Miltenyi Biotec, Auburn, CA) was used according to manufacturer's protocol to sort Sca-1 enriched and Sca-1 depleted fractions of isolated ear mesenchymal stem cells. Briefly, up to 10^7 cells ($p = 0$) were initially labeled with 10 μ l anti-Sea-1-FITC followed by magnetic labeling with 20 μ l anti-FITC MicroBeads. The cell suspension was then transferred to a MACS Column® placed in the magnetic field of a MACS Separator. Unlabeled (Sca-1⁻) cells were eluted with a buffer (PBS with 0.5% BSA and 2mM EDTA). The column was removed from the separator and retained Sca-1⁺ cells were flushed out with the buffer. The purity of each fraction was analyzed using flow cytometer (Becton Dickinson, San Jose, CA) as previously described [2].

Cell Doubling Assay

Cells were seeded in 96-well plate at a density of 5×10^4 /well. On day 1 and 4 the cells were fixed with 10% formaline for 1 h at RT followed by staining with 300 nM DAPI (Invitrogen, Carlsbad, CA) for 10 min at RT. Stained nuclei were visualized using a Nikon Eclipse TE2000-U (Nikon Instruments Inc., NY) inverted microscope equipped with a CoolSnap camera. Images of random fields were acquired with Metamorph imaging software (Molecular Devices Corp, Sunnyvale, CA), and cells were counted using image analysis software (ImageJ – <http://rsb.info.nih.gov/ij/>). Cell-doubling times (DT) were calculated according to the following formula [31]:

$$DT = \frac{CT}{\ln(N_f/N_i)/\ln(2)}$$

where DT is the cell-doubling time, CT the cell culture time, N_f the final number of cells, N_i the initial number of cells.

In Vitro Adipogenic Differentiation

Cells were replated in 6- or 12-well culture plates (Corning, Corning, NY) at the density of 10^4 /cm² and maintained in complete medium until confluent (considered as a day 0). Thereafter, the cells were exposed to an adipogenic induction medium containing DMEM/F12, 5% FBS, 1% antibiotic solution, 0.5 mM isobutylmethylxanthine, 1.7 μ M insulin and 1 μ M dexamethasone for 2 days (Adipogenic Medium I). For the next 7 days, medium was changed to DMEM/F12 supplemented with 5% FBS, 1% antibiotic solution, 17 nM insulin and 2 μ M thiazolidinedione (Adipogenic Medium II). On days 0, 3, 6 and 9, cells were harvested for RNA and protein purification, whereas culture media were collected for leptin assay.

Loss-of-Function Experiment

Sca-1 morpholino antisense oligonucleotides (Sca-1 MO) used in this study were designed and synthesized by Gene Tools, LLC Philomath, OR (www.gene-tools.com) based on the cDNA sequence of Sca-1 (Ly6a/E; GI:31981636). The morpholino sequence against the Sca-1 mRNA was 5'CTT TGT AGT GTG AGA AGT GTC CAT C3'. An irrelevant morpholino (standard control MO) and FITC-labeled standard control MOs were also purchased from Gene Tools. The MOs were prepared at a stock concentration of 500 μ M. EMSC were cultured in 6-well plates in DMEM/F12 media with 15% FBS. Subconfluent cells were treated with morpholino

oligos and Endo-Porter in DMEM/F12 media with 5% FBS (Day -1; see Fig. 2A). At Day 0 Adipogenic Medium I was added to the culture. After 48 hours medium was changed to Adipogenic Medium II. At Day 3, morpholino oligos and Endo-Porter were added a second time to the culture. Every third day during this process, selected cultures were removed for biochemical/morphological analysis by staining with Oil red O. In addition, total RNA and protein were isolated from similar cultures to measure marker gene expression by real time RT-PCR and Western Blot, respectively.

RNA Isolation and Quantitative Real-Time Reverse Transcriptase Polymerase Chain Reaction

Total RNA was extracted using Trizol (Invitrogen, Carlsbad, CA) and column-purified with RNeasy and RNase-Free DNase kits (Qiagen, Valencia, CA). cDNA synthesis was performed with 500 ng of total RNA using the High Capacity cDNA Archive Kit (Applied Biosystems, Foster City, CA). Endogenous mRNA levels for Sca-1, Pref-1, Wnt-10b, C/EBP β , CEBP δ , C/EBP α , PPAR γ 2, aP2, LPL and leptin were measured with Applied Biosystems Taqman[®] Gene Expression Assays (Applied Biosystems, Foster City, CA). Reactions were performed in MicroAmp Optic 384-well Reaction Plates (Applied Biosystems) using the ABI Prism 7900 Sequence Detection System (Perkin Elmer, Boston, MA) with the condition of 2 min at 48°C, 10 min at 95°C and then 40 cycles of 15 s at 95°C and 1 min at 60°C. The quantitative real-time polymerase chain reaction (qPCR) was performed in duplicate for each sample, and each run included a standard curve, non-template control, and negative RT control. Levels of gene expression were quantified relative to the level of hypoxanthine phosphoribosyltransferase 1 (HPRT1) using a standard curve method. HPRT1 was chosen as the internal control gene based on published [32] and our own data. Our preliminary qRT-PCR experiments did not show a significant difference in the mean levels of HPRT1 and GAPDH expression between Day 0 and Day 9 of adipogenic differentiation (data not shown). However, since the standard deviation (SD) of the HPRT1 gene was much tighter than that of GAPDH, we selected HPRT1 as our housekeeping gene for following studies.

Western Blot

Total cell lysates were prepared by adding 400 μ l of RIPA buffer containing protease inhibitor cocktail (Sigma-Aldrich, St. Louis, MO) and phosphatase inhibitor cocktails I and II (Sigma-Aldrich, St. Louis, MO). Total protein (40 μ g) was separated on 20% SDS-polyacrylamide gels under non-reducing conditions and transferred onto PVDF membranes (Millipore, Billerica, MA). The blots were then incubated with monoclonal antibodies against Sca-1 (eBioscience, San Diego, CA) diluted to a concentration of 1:100. Bands were visualized using the Odyssey imaging system (LI-COR Bioscience, San Diego, CA) with fluorescent (IRDye800TM or Cy5.5) labeled secondary antibodies according to the manufacturers' protocols.

Leptin Concentration in Medium

Adipogenic differentiation media were collected on Day 0, 3, 6 and 9. Leptin concentrations were determined using the DuoSet ELISA Development kit (R&D Systems Inc., Minneapolis, MN) according to manufacturer's protocol. Briefly, a 96-well plate was coated with 100 μ l Capture Antibody and incubated overnight at RT. Next, 100 μ l Detection Antibody was added to 100 μ l sample or standard. After a 2-h incubation, 100 μ l working dilution of Streptavidin-HRP was added for 20 min followed by incubation with 100 μ l Substrate Solution. The reaction was terminated with 50 μ l Stop Solution. The optical density of each well was read at 450 nm with wavelength correction at 540 nm. The concentration was calculated with a standard curve.

Oil Red O Staining

Differentiated cells were fixed for 1 h in 10% formalin at room temperature and later stained for lipid accumulation for 20 min with Oil red O. Cells were washed 3 times with water and observed under a phase contrast microscope. The dye retained by cells was eluted with isopropanol followed by absorbance measurements at 500 nm [33].

BODIPY/DAPI Staining

Differentiated cells were fixed with 10% formalin for 1 h at RT followed by staining with 300 nM DAPI 10 μ g/ml BODIPY® 493/503 (Invitrogen, Carlsbad, CA) in PBS for 20 min at RT. After washing 3 \times 5 min in PBS, cells were imaged with a Plan Fluor DL 10 \times objective using a Nikon Eclipse TE2000-U inverted microscope equipped with a CoolSnap camera. Images of random areas were captured and stored with Metamorph imaging software. Total area of BODIPY-stained lipid droplets (relative to a number of DAPI-stained nuclei) was measured using ImageJ image analysis software. Results are expressed as pixels per cell.

Sca-1 KO vs. C57BL/6J experiment

Sca-1 KO breeding pairs (C57BL/6J background [27]) were a kind gift from William L. Stanford (Institute of Biomaterials and Biomedical Engineering, University of Toronto, Toronto, Canada). Three weeks old Sca-1 KO (n = 10) and C57BL/6J (n = 10) mice were used for experiment. EMSC were isolated from 4-mm ear punches obtained during standard procedure used for marking live animals. Cells were harvested and cultured as described previously [2]. *In vitro* adipogenic differentiation was performed on cells from passage 2 seeded in 96-well plate. The cells were exposed to an adipogenic induction medium followed by BODIPY/DAPI staining and image analyzing as described above.

Statistical Analysis

Data expressed as mean \pm SD were analyzed with a two-tailed Student's test. A value of $p < 0.05$ was considered statistically significant.

RESULTS

Our previous study revealed that EMSC undergo robust adipogenic differentiation [1]. Additionally, flow cytometric analyses showed that undifferentiated EMSC are highly positive (82.77% \pm 7.8%) for Sca-1 [2]. The present experiments were undertaken to test the hypothesis that Sca-1 plays a role in adipogenic differentiation.

Sca-1⁺ cells display enhanced adipocyte differentiation capacity

Flow cytometric analysis of immunomagnetically sorted cells, revealed that 96.36% \pm 3.52% of EMSC in the Sca-1 enriched fraction and 12.06% \pm 9.06% in Sca-1 depleted fraction expressed Sca-1 (n = 18). Those data were confirmed by parallel analyses of Sca-1 mRNA content in both EMSC fractions (Fig. 1). Our next experiment asked whether there are differences in the proliferation rate of Sca-1 enriched vs. Sca-1 depleted EMSC fractions. The doubling times calculated for both fractions showed no statistical difference (2.72 \pm 1.08 vs. 3.19 \pm 1.33, respectively; $p = 0.5189$; Fig. 2). Further studies compared the adipogenic capacity of Sca-1 enriched and Sca-1 depleted fractions cultured under identical conditions. Following the induction of adipogenic differentiation, the expression of Sca-1 in both fractions was downregulated (see Fig. 1). The mRNA levels of negative regulators of adipocyte differentiation, Pref-1 (Fig. 3A) and Wnt-10b (Fig. 3B), were elevated in the undifferentiated EMSC (Day 0) and downregulated following adipogenic stimulation (Day 3, 6 and 9). The expression of the transcription factors C/EBP β (Fig. 3C) and C/EBP δ (Fig. 3D) showed similar patterns, with the highest expression at Day 0 that decreased during the course of the

differentiation process (Days 3–9). In contrast, the mRNAs encoding the adipogenic C/EBP α and PPAR γ 2 transcription factors were at low abundance on Day 0 but were significantly upregulated following adipogenic stimulation (Figs. 3E, 3F). The mRNA encoding late markers of adipogenic differentiation, LPL and aP2, showed similar patterns of expression – low on Day 0 followed by significant induction during subsequent days of differentiation (Figs. 3G, 3H). Comparative analysis of the adipogenic differentiation process between Sca-1 enriched and Sca-1 depleted populations of EMSC revealed substantial differences in the genes expression. Pref-1, C/EBP β , C/EBP α , PPAR γ 2, LPL and aP2 were expressed at significantly higher levels in the Sca-1 enriched EMSC fraction. However, leptin expression displayed the most striking difference between the Sca-1 enriched and Sca-1 depleted EMSC fractions during adipogenic differentiation (Fig. 3I and 3J). Whereas the Sca-1⁺ fraction showed a time-dependent and substantial increase in leptin mRNA, the Sca-1 depleted fraction expressed leptin at low levels with no change in its expression between Day 3 and Day 9 (Fig. 3I). Moreover, leptin secretion measured in conditioned media was detected only in Sca-1 enriched EMSC (Fig. 3J). To compare morphological changes and neutral lipid accumulation, cells from both fractions were stained with Oil red O or BODIPY on Day 0 and Day 9 of differentiation (Fig. 4 A–4D). Based on Oil red O, lipid accumulation was much denser in Sca-1 enriched cells (compare Fig. 4B and Fig. 4C) and this difference was statistically significant (0.72 ± 0.02 and 0.58 ± 0.09 ; $p < 0.001$; Fig. 4A). Based on BODIPY staining, the ratio of lipid droplets relative to the number of DAPI-stained nuclei was greater in the Sca-1 enriched EMSC population by a factor of 1.48 ($p < 0.05$; Fig. 4D).

The lower adipogenic potential of Sca-1 negative fraction additionally has been confirmed by using EMSC isolated from our recently established Sca-1^{-/-} mouse colony (C57BL/6J genetic background). From our limited number of Sca1 KO animals we collected ear punches and used these 4 mm diameter tissues to isolate EMSC from live animals [2]. The EMSC isolated from Sca-1^{-/-} mice and exposed to adipogenic cocktails showed a significantly lower ($p < 0.01$) accumulation of BODIPY-stained lipid droplets relative to DAPI-stained nuclei relative to EMSC derived from wild type C57BL/6J mice (Fig. 4E).

Sca-1 Morpholino Knockdown Has No Effect on EMSC Adipogenic Differentiation

Morpholino oligonucleotides (MO) do not cause degradation of their RNA targets but reduce their biological activity through post-transcriptional mechanisms. Consequently, Western Blot analyses of protein levels rather than RT-PCR analyses of mRNA levels are the most suitable assay of MO activity and effectiveness. As a first step to estimate the efficacy of our Sca-1 MO, we performed Western Blot analysis of Sca-1 expression during EMSC adipogenic differentiation (Fig. 5A). The temporal analysis revealed a low expression of Sca-1 protein on Day -1 in non-confluent cells that increased on Day 0 at confluence and was sustained during subsequent first two days of adipogenic differentiation. A gradual decrease in Sca-1 protein expression was observed between Day 3 and Day 9 of differentiation.

To estimate the optimal efficacy of Sca-1 MO, EMSC at sub-confluent (Day -1) or Day 3 of differentiation were treated with increasing concentrations of MO and its delivery component (Endo-Porter; Gene Tools, LLC) (Fig. 5B). Based on Western blot analysis of Sca-1 expression and on microscopic appearance of cells, we identified the optimal concentrations of Sca-1 MO and Endo-Porter to be 1 μ M and 6 μ M, respectively (Fig. 5B). Once the effectiveness of the Sca-1 MO was established, we further tested the role of Sca-1 in adipogenic differentiation by determining whether blocking of Sca-1 expression in EMSC alters their adipogenic capacity. EMSC were treated with Sca-1 MO or a scrambled control MO on Days -1 and 3 of the differentiation procedure. The Western Blot data (Fig. 5C) documented inhibition of Sca-1 protein expression in Sca-1 MO treated cells on Day 3, 6 and 9 of differentiation. However, spectrophotometric analysis of Oil red O staining (Fig. 5E) and adipogenic morphology (data

not shown) showed no differences between Sca-1MO and control scrambled MO treated cultures. The differentiation of EMSC into adipocytes was verified by qRT-PCR of Pref-1, Wnt10b, PPAR γ 2, aP2, LPL and leptin in total RNA from control MO and Sca-1MO treated cultures (Fig. 5D). Gene expression analyses revealed no differences between Sca-1 MO and control MO treated cultures.

DISCUSSION

The present study shows that Sca-1 enriched and Sca-1 depleted population of EMSC differ in their capacity to differentiate into adipocytes. This conclusion is based on quantitative measures of neutral lipid accumulation as well as by the expression of mRNAs encoding adipogenic transcription factors. Furthermore, a disparity in leptin secretion has been noted.

The epidermal growth factor-related surface protein, Preadipocyte Factor 1 (Pref-1), also known as delta-like protein 1 (dlk-1), plays a role in maintaining preadipocytes in their undifferentiated state [34,35]. Pref-1 expression is repressed when preadipocytes are induced to differentiate, and overexpression of the gene inhibits adipocyte differentiation [36]. Similarly, Wnt10b has been demonstrated to inhibit adipogenic differentiation [37,38] and disruption of its extracellular signaling results in spontaneous adipocyte conversion *in vitro*. In the present study, the expression of both Pref-1 and Wnt10b mRNA were suppressed upon induction of EMSC differentiation.

Members of the CCAAT enhancer binding protein (C/EBP) family of transcription factors have long been recognized as serving a critical role in adipogenic differentiation [39]. In our study, the C/EBP expression pattern of the EMSC mirrored those reported in studies of 3T3-L1 preadipocytes – expression of C/EBP β and C/EBP δ preceded both C/EBP α and PPAR γ [40,41], which together induce expression of the complement of genes necessary to create the adipocyte phenotype.

PPAR γ , a member of peroxisome proliferator-activated receptor family of nuclear hormone receptors, is recognized as serving a central role in the regulation of adipogenesis [42,43]. PPAR γ 2 is the predominant isoform found in adipocytes and its expression, as along with that of late adipogenic markers (LPL and aP2), was upregulated during the course of differentiation.

The most significant difference between Sca-1 enriched and Sca-1 depleted EMSC was their expression of leptin, at both the mRNA and protein level. Despite the fact that Sca-1 depleted EMSC accumulated lipid droplets, their leptin mRNA content remained very low following adipogenic induction, and their secreted leptin protein level was undetectable. These observations may suggest that Sca-1 plays a positive role in leptin secretion; however, EMSC depleted of Sca-1 by morpholino treatment did not show down-regulation of leptin secretion. Thus, the data suggest the existence of two different types of stem cells/preadipocyte precursors. The first exhibits Sca-1 positivity and gives rise to fully functional adipocytes while the second one is Sca-1 negative and less capable of adipocyte differentiation. Studies from the literature support this hypothesis since preadipocytes isolated from different fat depots display different adipogenic potential [44,45]. For example, Tchkonina et al. [46] showed that there are substantial differences between preadipocytes from mesenteric and omental visceral depots, based on their gene expression profiles and capacity for replication and adipogenesis. Likewise, substantial differences exist in leptin and adiponectin genes expression between porcine intramuscular and subcutaneous adipocytes [47]. Our observations regarding the enhanced adipogenic capacity of Sca-1 expressing EMSC are consistent with previously published data. Colony-forming unit adipocyte assays have determined that Sca-1^{-/-} bone marrow-derived cells formed 50% fewer colonies compared to Sca-1^{+/+} cultures [26]. An independent study showed diverse, age-dependent adipogenic differentiation of mesenchymal

progenitors derived from Sca-1^{-/-} vs. Sca-1^{+/+} mice. Bone marrow-derived cells from the Sca-1^{+/+} mice exhibited significantly greater numbers of spontaneously differentiating Oil red O-stained colonies at the age of 7 and 9 months. In contrast, younger mice (3 and 5 mo of age) showed no significant difference; marrow-derived cells from both Sca-1^{+/+} and Sca-1^{-/-} displayed a limited capacity to form adipogenic colonies in the absence of adipogenic stimuli [48]. Although our study used young mice (3–6 wk of age), we added adipogenic inductive cocktails to the EMSC at confluence. Thus, both exogenous and tissue specific paracrine factors may account for the difference in our current findings and those in the literature. Consistent with our report, a higher adipogenic potential was reported in the Sca-1⁺ fraction of cells isolated from fetal mouse calvaria; this study likewise employed an adipogenic inductive cocktail over a 21 day period [49]. Additionally, significantly higher PPAR γ expression was determined in Sca-1⁺ calvarial cells compared to Sca-1⁻ cells [44].

While Sca-1⁻ cells may have a limited adipogenic capacity, they can differentiate along other lineage pathways. Steenhuis et. al showed that cells from fetal mouse calvaria within the Sca-1⁻ fraction have higher chondrogenic and osteogenic potential relative to the Sca-1⁺ fraction [49]. These authors observed positive alkaline phosphatase staining primarily in the Sca-1⁻ fraction following chondrogenic differentiation and only Sca-1⁻ cells exhibited mineralization when exposed to osteogenic medium [49]. Likewise, Sca-1⁻ cells have been found to display more efficient myogenic differentiation [28]. C2C12 myogenic Sca-1⁻ cells formed myotubes robustly, whereas myotube formation by Sca-1⁺ cells was not observed [28]. These findings and parallel gain-of-function/loss-of-function experiments have led to the suggestion that Sca-1 expression not only defines a subpopulation of muscle cells that are restricted to the myogenic lineage, but also serves a functional role by regulating myoblast proliferation and myogenic differentiation.

In summary, Sca1 is an intriguing marker that selects for EMSC with enhanced adipogenic potential. Further studies, using the Sca1^{-/-} murine model, will explore what role, if any, this surface antigen plays in regulating EMSC adipocyte commitment and differentiation.

ACKNOWLEDGMENTS

We thank Marilyn Dietrich for flow cytometry analysis, Tamra Mendoza for assisting with animal husbandry, and William Stanford for providing the Sca-1^{-/-} murine model.

This work was supported by National Institutes of Health; Grant number: RO1 1 P20 RR021945 COBRE.

REFERENCES

1. Gawronska-Kozak B. Regeneration in the ears of immunodeficient mice: identification and lineage analysis of mesenchymal stem cells. *Tissue Eng* 2004;10:1251–1265. [PubMed: 15363180]
2. Gawronska-Kozak B, Manuel JA, Prpic V. Ear mesenchymal stem cells (EMSC) can differentiate into spontaneously contracting muscle cells. *J Cell Biochem* 2007;102:122–135. [PubMed: 17370316]
3. Rim JS, Mynatt RL, Gawronska-Kozak B. Mesenchymal stem cells from the outer ear: a novel adult stem cell model system for the study of adipogenesis. *Faseb J* 2005;19:1205–1207. [PubMed: 15857881]
4. Gumley TP, McKenzie IF, Sandrin MS. Tissue expression, structure and function of the murine Ly-6 family of molecules. *Immunology & Cell Biology* 1995;73:277–296. [PubMed: 7493764]
5. Baddoo M, Hill K, Wilkinson R, et al. Characterization of mesenchymal stem cells isolated from murine bone marrow by negative selection. *J Cell Biochem* 2003;89:1235–1249. [PubMed: 12898521]
6. Gojo S, Gojo N, Takeda Y, et al. In vivo cardiovascularogenesis by direct injection of isolated adult mesenchymal stem cells. *Exp Cell Res* 2003;288:51–59. [PubMed: 12878158]

7. Lee J, Kuroda S, Shichinohe H, et al. Migration and differentiation of nuclear fluorescence-labeled bone marrow stromal cells after transplantation into cerebral infarct and spinal cord injury in mice. *Neuropathology* 2003;23:169–180. [PubMed: 14570283]
8. Peister A, Mellad JA, Larson BL, et al. Adult stem cells from bone marrow (MSCs) isolated from different strains of inbred mice vary in surface epitopes, rates of proliferation, and differentiation potential. *Blood* 2004;103:1662–1668. [PubMed: 14592819]
9. Gussoni E, Soneoka Y, Strickland CD, et al. Dystrophin expression in the mdx mouse restored by stem cell transplantation. *Nature* 1999;401:390–394. [PubMed: 10517639]
10. Welm BE, Tepera SB, Venezia T, et al. Sca-1(pos) cells in the mouse mammary gland represent an enriched progenitor cell population. *Dev Biol* 2002;245:42–56. [PubMed: 11969254]
11. Matsuura K, Nagai T, Nishigaki N, et al. Adult cardiac Sca-1-positive cells differentiate into beating cardiomyocytes. *J Biol Chem* 2004;279:11384–11391. [PubMed: 14702342]
12. Montanaro F, Liadaki K, Volinski J, et al. Skeletal muscle engraftment potential of adult mouse skin side population cells. *Proc Natl Acad Sci U S A* 2003;100:9336–9341. [PubMed: 12886022]
13. Asakura A. Stem cells in adult skeletal muscle. *Trends Cardiovasc Med* 2003;13:123–128. [PubMed: 12691677]
14. Benchaouir R, Rameau P, Decraene C, et al. Evidence for a resident subset of cells with SP phenotype in the C2C12 myogenic line: a tool to explore muscle stem cell biology. *Exp Cell Res* 2004;294:254–268. [PubMed: 14980519]
15. Jankowski RJ, Haluszczak C, Trucco M, et al. Flow cytometric characterization of myogenic cell populations obtained via the preplate technique: potential for rapid isolation of muscle-derived stem cells. *Hum Gene Ther* 2001;12:619–628. [PubMed: 11426462]
16. Lee JY, Qu-Petersen Z, Cao B, et al. Clonal isolation of muscle-derived cells capable of enhancing muscle regeneration and bone healing. *J Cell Biol* 2000;150:1085–1100. [PubMed: 10973997]
17. Majka SM, Jackson KA, Kienstra KA, et al. Distinct progenitor populations in skeletal muscle are bone marrow derived and exhibit different cell fates during vascular regeneration. *J Clin Invest* 2003;111:71–79. [PubMed: 12511590]
18. Tamaki T, Akatsuka A, Ando K, et al. Identification of myogenic-endothelial progenitor cells in the interstitial spaces of skeletal muscle. *J Cell Biol* 2002;157:571–577. [PubMed: 11994315]
19. Blake PG, Madrenas J, Halloran PF. Ly-6 in kidney is widely expressed on tubular epithelium and vascular endothelium and is up-regulated by interferon gamma. *J Am Soc Nephrol* 1993;4:1140–1150. [PubMed: 8305641]
20. Falcatori I, Borsellino G, Haliassos N, et al. Identification and enrichment of spermatogonial stem cells displaying side-population phenotype in immature mouse testis. *Faseb J* 2004;18:376–378. [PubMed: 14688197]
21. Petersen BE, Grossbard B, Hatch H, et al. Mouse A6-positive hepatic oval cells also express several hematopoietic stem cell markers. *Hepatology* 2003;37:632–640. [PubMed: 12601361]
22. Wulf GG, Luo KL, Jackson KA, et al. Cells of the hepatic side population contribute to liver regeneration and can be replenished with bone marrow stem cells. *Haematologica* 2003;88:368–378. [PubMed: 12681963]
23. Burger PE, Xiong X, Coetzee S, et al. Sca-1 expression identifies stem cells in the proximal region of prostatic ducts with high capacity to reconstitute prostatic tissue. *Proc Natl Acad Sci U S A* 2005;102:7180–7185. [PubMed: 15899981]
24. Xin L, Lawson DA, Witte ON. The Sca-1 cell surface marker enriches for a prostate-regenerating cell subpopulation that can initiate prostate tumorigenesis. *Proc Natl Acad Sci U S A* 2005;102:6942–6947. [PubMed: 15860580]
25. Kotton DN, Summer RS, Sun X, et al. Stem cell antigen-1 expression in the pulmonary vascular endothelium. *Am J Physiol Lung Cell Mol Physiol* 2003;284:L990–L996. [PubMed: 12611818]
26. Bonyadi M, Waldman SD, Liu D, et al. Mesenchymal progenitor self-renewal deficiency leads to age-dependent osteoporosis in Sca-1/Ly-6A null mice. *Proc Natl Acad Sci U S A* 2003;100:5840–5845. [PubMed: 12732718]
27. Ito CY, Li CY, Bernstein A, et al. Hematopoietic stem cell and progenitor defects in Sca-1/Ly-6A-null mice. *Blood* 2003;101:517–523. [PubMed: 12393491]

28. Mitchell PO, Mills T, O'Connor RS, et al. Sca-1 negatively regulates proliferation and differentiation of muscle cells. *Dev Biol* 2005;283:240–252. [PubMed: 15901485]
29. Qu-Petersen Z, Deasy B, Jankowski R, et al. Identification of a novel population of muscle stem cells in mice: potential for muscle regeneration. *J Cell Biol* 2002;157:851–864. [PubMed: 12021255]
30. Wolnicka-Glubisz A, King W, Noonan FP. SCA-1+ cells with an adipocyte phenotype in neonatal mouse skin. *J Invest Dermatol* 2005;125:383–385. [PubMed: 16098051]
31. Rainaldi G, Pinto B, Piras A, et al. Reduction of proliferative heterogeneity of CHEF18 Chinese hamster cell line during the progression toward tumorigenicity. *In Vitro Cellular & Developmental Biology* 1991;27A:949–952. [PubMed: 1757399]
32. Vandesompele J, De Preter K, Pattyn F, et al. Accurate normalization of real-time quantitative RT-PCR data by geometric averaging of multiple internal control genes. *Genome Biol* 2002;3RESEARCH0034
33. Halvorsen YD, Franklin D, Bond AL, et al. Extracellular matrix mineralization and osteoblast gene expression by human adipose tissue-derived stromal cells. *Tissue Eng* 2001;7:729–741. [PubMed: 11749730]
34. Smas CM, Green D, Sul HS. Structural characterization and alternate splicing of the gene encoding the preadipocyte EGF-like protein pref-1. *Biochemistry* 1994;33:9257–9265. [PubMed: 7519443]
35. Smas CM, Sul HS. Pref-1, a protein containing EGF-like repeats, inhibits adipocyte differentiation. *Cell* 1993;73:725–734. [PubMed: 8500166]
36. Smas CM, Chen L, Sul HS. Cleavage of membrane-associated pref-1 generates a soluble inhibitor of adipocyte differentiation. *Molecular & Cellular Biology* 1997;17:977–988. [PubMed: 9001251]
37. Bennett CN, Ross SE, Longo KA, et al. Regulation of Wnt signaling during adipogenesis. *J Biol Chem* 2002;277:30998–31004. [PubMed: 12055200]
38. Ross SE, Hemati N, Longo KA, et al. Inhibition of adipogenesis by Wnt signaling. *Science* 2000;289:950–953. [PubMed: 10937998]
39. McKnight SL, Lane MD, Gluecksohn-Waelsch S. Is CCAAT/enhancer-binding protein a central regulator of energy metabolism? *Genes & Development* 1989;3:2021–2024. [PubMed: 2697636]
40. Cao Z, Umek RM, McKnight SL. Regulated expression of three C/EBP isoforms during adipose conversion of 3T3-L1 cells. *Genes & Development* 1991;5:1538–1552. [PubMed: 1840554]
41. Yeh WC, Cao Z, Classon M, et al. Cascade regulation of terminal adipocyte differentiation by three members of the C/EBP family of leucine zipper proteins. *Genes & Development* 1995;9:168–181. [PubMed: 7531665]
42. Brun RP, Spiegelman BM. PPAR gamma and the molecular control of adipogenesis. *J Endocrinol* 1997;155:217–218. [PubMed: 9415052]
43. Spiegelman BM, Hu E, Kim JB, et al. PPAR gamma and the control of adipogenesis. *Biochimie* 1997;79:111–112. [PubMed: 9209705]
44. Lefebvre AM, Laville M, Vega N, et al. Depot-specific differences in adipose tissue gene expression in lean and obese subjects. *Diabetes* 1998;47:98–103. [PubMed: 9421381]
45. Tchkonja T, Tchoukalova YD, Giorgadze N, et al. Abundance of two human preadipocyte subtypes with distinct capacities for replication, adipogenesis, and apoptosis varies among fat depots. *Am J Physiol Endocrinol Metab* 2005;288:E267–E277. [PubMed: 15383371]
46. Tchkonja T, Lenburg M, Thomou T, et al. Identification of depot-specific human fat cell progenitors through distinct expression profiles and developmental gene patterns. *Am J Physiol Endocrinol Metab* 2007;292:E298–E307. [PubMed: 16985259]
47. Gardan D, Gondret F, Louveau I. Lipid metabolism and secretory function of porcine intramuscular adipocytes compared with subcutaneous and perirenal adipocytes. *Am J Physiol Endocrinol Metab* 2006;291:E372–E380. [PubMed: 16705057]
48. Holmes C, Khan TS, Owen C, et al. Longitudinal analysis of mesenchymal progenitors and bone quality in the stem cell antigen-1-null osteoporotic mouse. *Journal of Bone & Mineral Research* 2007;22:1373–1386. [PubMed: 17547535]
49. Steenhuis P, Pettway GJ, Ignelzi MA Jr. Cell surface expression of stem cell antigen-1 (sca-1) distinguishes osteo-, chondro-, and adipoprogenitors in fetal mouse calvaria. *Calcif Tissue Int* 2008;82:44–56. [PubMed: 18175035]

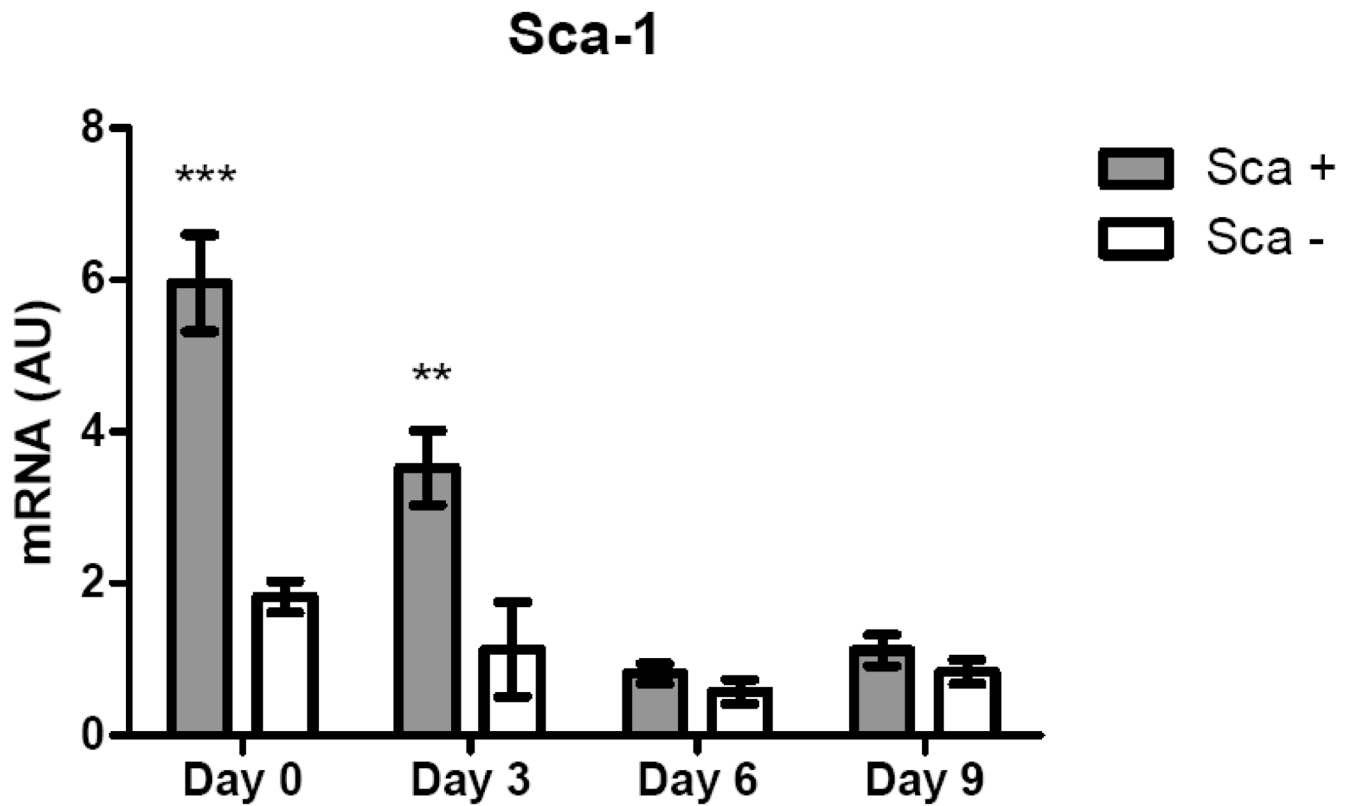


Figure 1. Real time RT-PCR analysis for Sca-1 expression in Sca-1 enriched and Sca-1 depleted fractions of EMSC during time course of adipogenic differentiation (***) $p < 0.001$; ** $p < 0.01$).

Cell Doubling Time

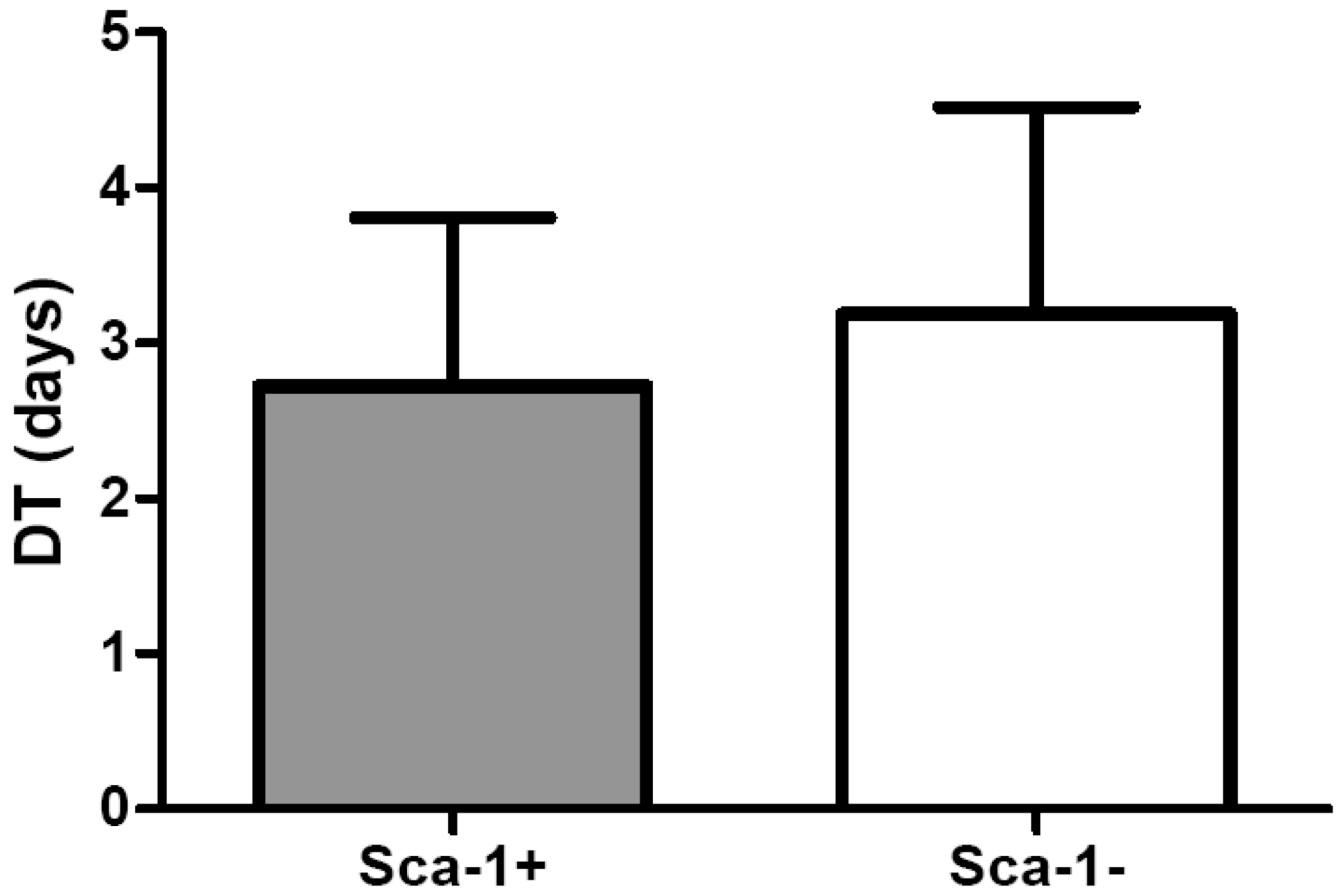


Figure 2. Cell doubling time of cultured Sca-1 enriched and Sca-1 depleted fractions of EMSC. The values reflect the mean \pm standard deviation.

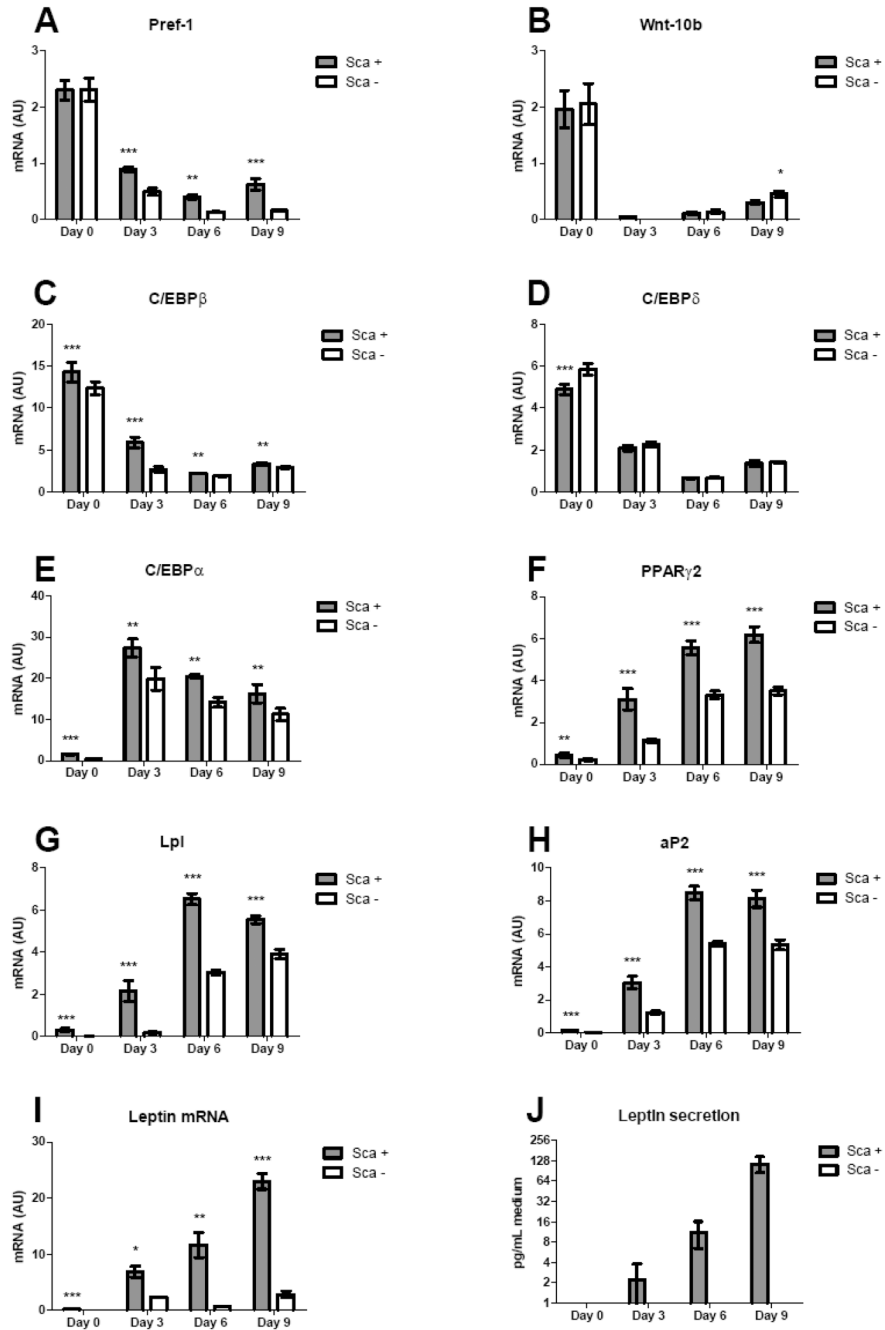


Figure 3. Sca-1 enriched population of EMSC displays enhanced adipocyte differentiation capacity. **A-I:** Gene expression profiles of Sca-1 enriched vs. Sca-1 depleted fractions of EMSC during adipogenic differentiation. **J:** Leptin protein secretion in cultured media. (* $p < 0.05$; ** $p < 0.01$; *** $p < 0.001$)

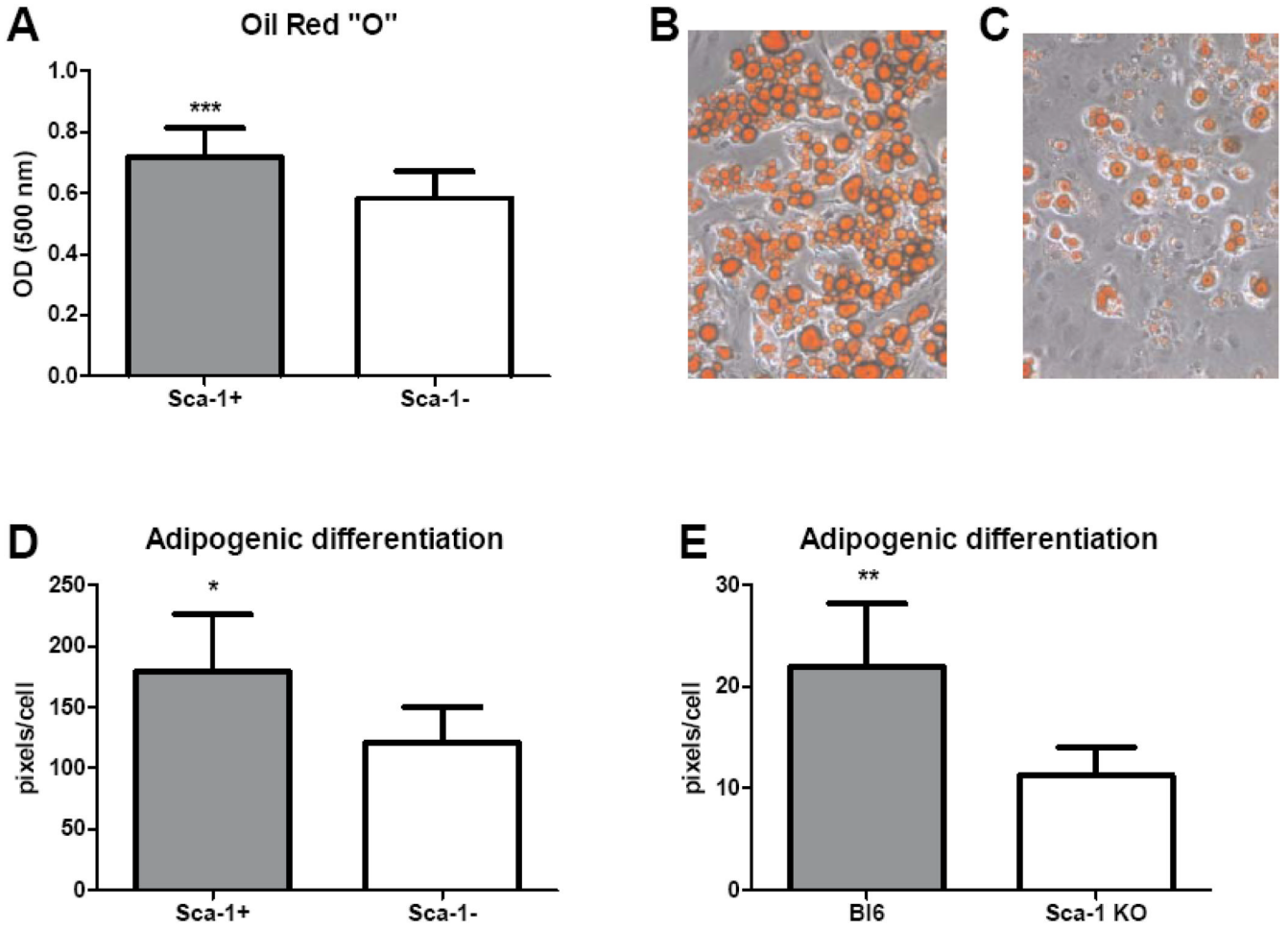
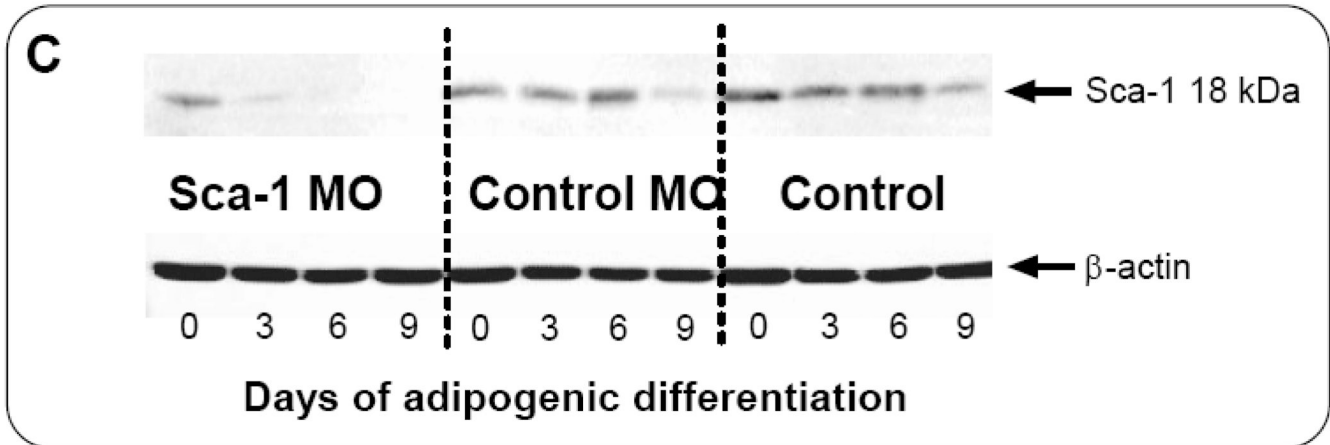
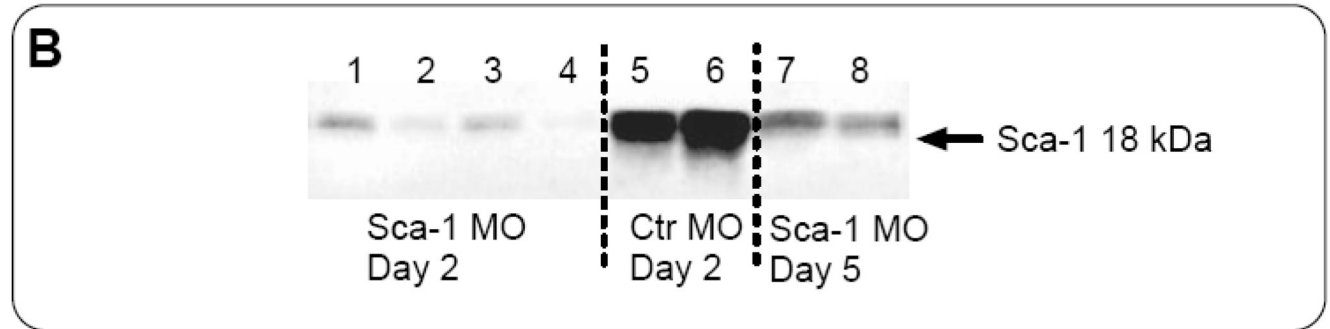
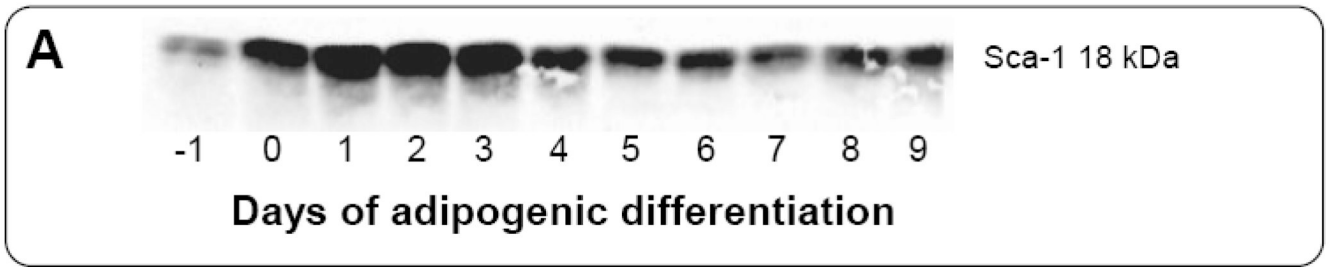
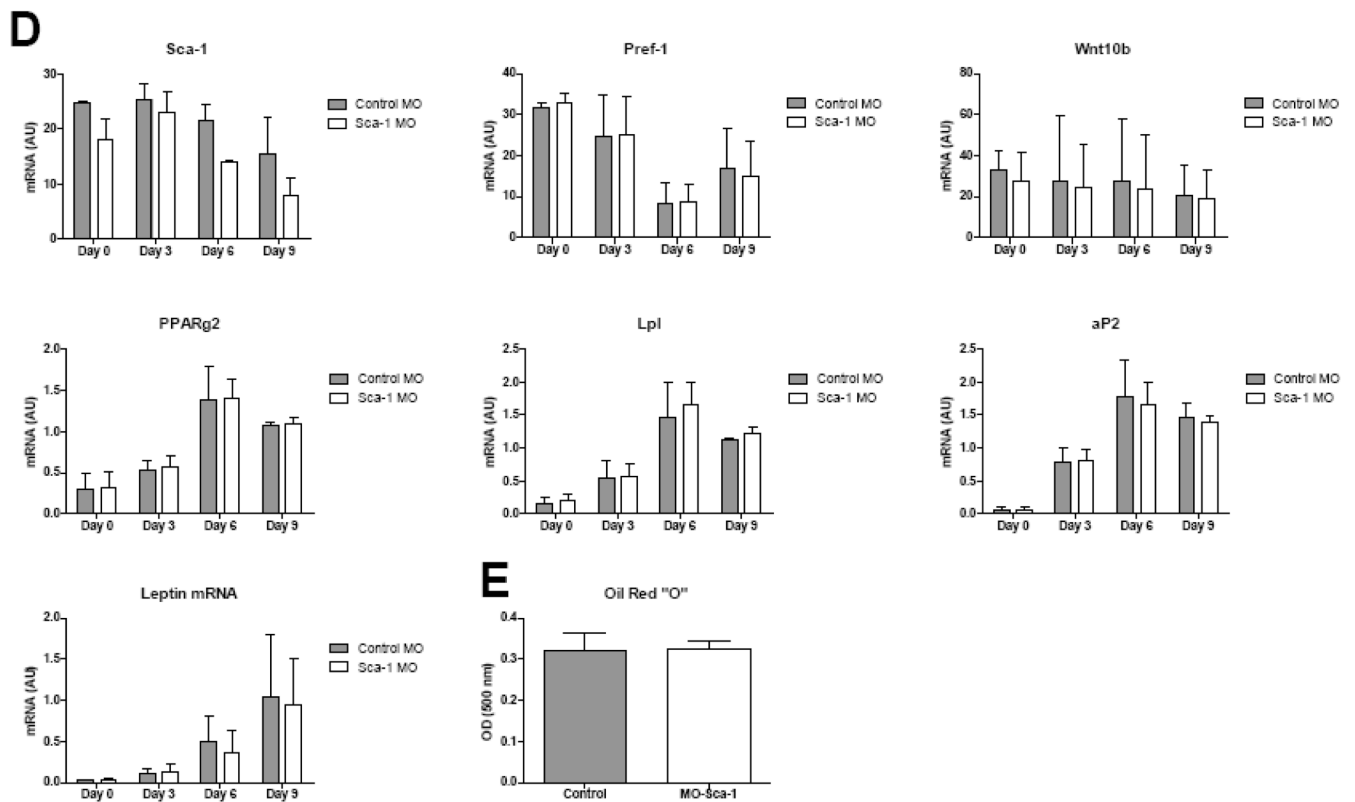


Figure 4. Adipogenic potentials of Sca-1 enriched vs. Sca-1 depleted EMSC (A-D), and C57BL/6J vs. Sca-1^{-/-} EMSC (E). **A:** Spectrophotometric analysis of Oil red O staining. **B** and **C:** Phase contrast micrographs of Sca-1 enriched (**B**) and Sca-1 depleted (**C**) cells at Day 9 of adipogenic differentiation. Image analyses of area of BODIPY-stained lipid droplets adjusted to the cell number of Sca-1 enriched vs. Sca-1 depleted cells (**D**), and C57BL/6J vs. Sca-1^{-/-} EMSC (**E**). (* $p < 0.05$; ** $p < 0.01$; *** $p < 0.001$)



**Figure 5.**

Sca-1 morpholino antisense oligonucleotides (Sca-1 MO) down-regulate Sca-1 expression in EMSC. **A, B:** Western Blot analysis of Sca-1 expression during EMSC adipogenic differentiation: (**A**) untreated EMSC, (**B**) MO treated EMSC. Sca-1 MO at Day 2 and Day 5 and control morpholino (Ctr MO) at Day 2. Line 1: Sca-1MO 1 μ M + Endo-Porter 2 μ M; line 2 Sca-1 MO 1 μ M+Endo-Porter 6 μ M; line 3 Sca-1 MO 10 μ M+Endo-Porter 2 μ M; line 4 Sca-1 MO10 μ M+Endo-Porter 6 μ M; line 5 control MO 1 μ M+Endo-Porter 2 μ M; line 5 control MO 1 μ M+Endo-Porter 6 μ M; line 7 Sca-1 MO1 μ M+Endo-Porter 2 μ M; line 8 Sca-1 MO 1 μ M+Endo-Porter 6 μ M. **C:** Western Blot analysis of Sca-1 expression on Days: 0, 3, 6, 9 of adipogenic differentiation in Sca-1 MO, Ctr MO treated and control/untreated cultures. **D:** Gene expression profiles of morpholino-treated EMSC. **E:** Spectrophotometric analysis of lipid droplet accumulation indicated by staining with Oil red O.